Comparative Analysis of Pump Sizing Requirements Molten Salt Systems

Sunghyun Yoo [a], Gihyeon Kim [a], Jeong Ik Lee[a*]
[a] *Dept. Nuclear & Quantum Eng., KAIST, 291 Daehak-ro, Yuseong-gu, Daejeon 34141, Republic of Korea*
[*] *Corresponding author: jeongiklee@kaist.ac.kr*

Keywords : Molten Salt, Pump design requirement, Affinity law, NaCl-$MgCl_2$, KCl-$MgCl_2$, LiF-BeF_2

1. Introduction

The rapid expansion of advanced technologies such as artificial intelligence (AI), high-performance computing, and electric vehicles (EVs) has led to an unprecedented increase in global electricity demand. Meeting this accelerating demand while simultaneously achieving carbon neutrality requires large-scale, reliable, and low-carbon energy sources. In this context, nuclear energy has re-emerged as a critical option for sustainable baseload power generation. In particular, Gen-IV reactor systems are receiving significant attention due to their enhanced safety, improved fuel utilization, and higher thermal efficiency compared to conventional light water reactors (LWRs).

Among the various Gen-IV concepts, the molten salt reactor (MSR) is considered one of the most promising designs because of its inherent safety characteristics, high operating temperature, and potential for superior thermal efficiency [1]. However, the thermophysical properties of molten salts—such as high density and relatively low specific heat capacity—differ substantially from those of water [2]. While previous studies have extensively examined neutronic behavior and heat transfer characteristics of MSRs, comparatively limited attention has been given to the hydraulic power requirements associated with coolant circulation. The pumping power demand may represent a non-negligible parasitic load that affects net plant efficiency.

To quantitatively assess this hydraulic penalty, the present study performs a comparative thermo-hydraulic analysis of water and three representative molten salt coolants under identical system conditions. A reference thermal power of 100 MW, temperature rise of 50 K, pipe length of 100 m, and pipe diameter of 0.5 m are imposed to ensure consistent comparison. For each fluid, mass flow rate, pump head, hydraulic power, Reynolds number, and scaling behavior based on pump affinity laws are evaluated. In addition, mechanical design implications are examined through impeller diameter and rotational speed scaling as well as specific speed estimation. By systematically linking coolant thermophysical properties to hydraulic performance and pump design parameters, this study aims to provide a quantitative foundation for evaluating circulation system requirements in molten salt reactor applications.

2. Methodology

2.1 System Definition

A steady-state single-phase forced circulation loop was considered to evaluate the hydraulic performance of different coolants. To ensure consistent comparison, identical geometric and thermal conditions were imposed for all fluids.

The reference thermal power was fixed at 100 MW, with a prescribed temperature rise of 50 K across the loop. The piping system was modeled as a straight circular pipe with a length of 100 m and an inner diameter of 0.5 m [3, 4]. Pump hydraulic efficiency was assumed to be 0.7. Gravitational acceleration was set to 9.81 m/s^2.

For the water case, to ensure single-phase operation at the defined hot-leg temperature of T_{hot} = 500 ℃, the system pressure was set to P_{water} = 25 MPa, which exceeds the critical pressure of water (22.064 MPa). Accordingly, water was treated as a single-phase supercritical fluid throughout the analysis. Although supercritical water exhibits strong property variations near the pseudo-critical region, such effects are neglected in the present study for comparative consistency, and constant thermophysical properties are assumed.

Fig. 1 illustrates a simplified schematic of the idealized circulation loop considered in this study.

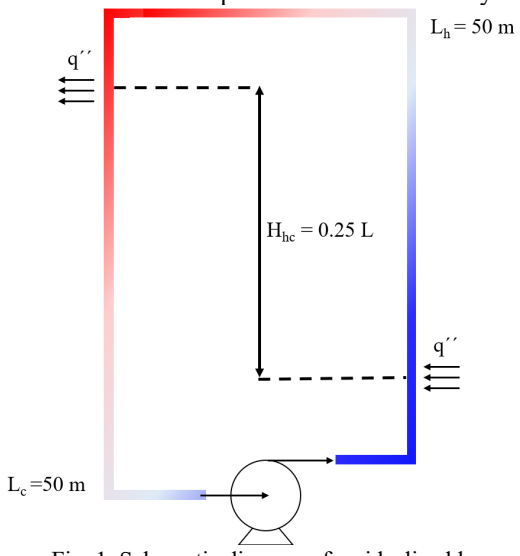

Fig. 1. Schematic diagram of an idealized loop

Four working fluids were analyzed: water and three representative molten salts (LiF–BeF_2 (FLiBe), KCl–$MgCl_2$, and NaCl–$MgCl_2$). Thermophysical properties were treated as constants for comparative evaluation. The density range of molten salts considered in this study was approximately 1870–1890 kg/m^3, while specific heat capacity ranged from 1080 to 2414 J/kg·K [5, 6]. The density and specific heat of water were evaluated based on the IAPWS-IF97 (International Association for the Properties of Water and Steam Industrial Formulation 1997), while the dynamic viscosity was calculated using the IAPWS viscosity correlation proposed by Huber et al [7].

2.2 Thermo-Hydraulic Formulation

The required mass flow rate for heat removal was determined from the steady-state energy balance:

$$\dot{m} = \frac{Q_{th}}{c_p \Delta T} \tag{1}$$

The volumetric flow rate and mean velocity were calculated as:

$$Q = \frac{\dot{m}}{\rho}, \qquad V = \frac{Q}{A_f} \tag{2}$$

where $A_f = \pi D^2/4$ is the pipe cross-sectional area.

The Reynolds number was evaluated as:

$$Re = \frac{\rho V D}{\mu} \tag{3}$$

For turbulent flow conditions, the Darcy friction factor was estimated using the Blasius correlation:

$$f = 0.316 Re^{-0.25} \tag{4}$$

Since all evaluated cases satisfy Re > 10^5 and the pipe is assumed hydraulically smooth, the Blasius correlation is considered applicable as a simplified turbulent friction model for comparative purposes.

The frictional head loss was calculated from the Darcy–Weisbach formulation:

$$\Delta P_{loss} = f \frac{L}{D} \frac{\rho V^2}{2} \tag{5}$$

The buoyancy-induced pressure difference due to density variation between hot and cold legs was evaluated as:

$$\Delta P_{buoy} = g H_{hc} (\rho_{cold} - \rho_{hot}) \tag{6}$$

The corresponding buoyancy head was calculated as:

$$H_{buoy} = \frac{\Delta P_{buoy}}{\rho g} \tag{7}$$

Where $H_{hc} = 0.25L$ represents the effective vertical height of the loop.

The net pump head required to sustain forced circulation was then defined as:

$$H_{pump} = H_{loss} - H_{buoy} \tag{8}$$

The pump power requirement was evaluated based on the net required head.

The required pump power was calculated based on the pressure drop and volumetric flow rate as:

$$P_{pump} = \frac{\Delta P Q}{\eta} \tag{9}$$

where η denotes the pump hydraulic efficiency, which was assumed to be 0.7 for all cases in this study. This formulation enables quantitative isolation of hydraulic performance variations attributable solely to differences in coolant thermophysical properties.

2.3 Pump Scaling and Mechanical Design Parameters

To evaluate the mechanical scaling requirements imposed by different coolant properties, classical pump affinity laws based on geometric similarity were applied [8-10]:

$$\left(\frac{Q}{ND^3}\right)_1 = \left(\frac{Q}{ND^3}\right)_2 \tag{10.a}$$

$$\left(\frac{H}{N^2D^2}\right)_1 = \left(\frac{H}{N^2D^2}\right)_2 \tag{10.b}$$

$$\left(\frac{P}{\rho N^2D^2}\right)_1 = \left(\frac{P}{\rho N^2D^2}\right)_2 \tag{10.c}$$

$$\left(\frac{\dot{W}}{\rho N^3D^5}\right)_1 = \left(\frac{\dot{W}}{\rho N^3D^5}\right)_2 \tag{10.d}$$

From these relations, the commonly used simplified scaling forms can be derived [8-10]:

$$Q \propto ND^3 \tag{11.a}$$

$$H \propto N^2D^2 \tag{11.b}$$

$$\dot{W} \propto \rho N^3D^5 \tag{11.c}$$

Using water as a reference case, relative impeller diameter and rotational speed ratios were derived for each fluid. Additionally, pump power was mapped in rotational speed–diameter (N–D) space to visualize design feasibility under varying operating conditions.

The specific speed was evaluated to examine pump type implications [8-10]:

$$N_s = \frac{N\sqrt{Q}}{H^{3/4}} \tag{12}$$

where *N* is the rotational speed in rpm. This parameter provides a dimensionless indicator of pump type suitability, distinguishing radial, mixed-flow, and axial-flow design regimes based on hydraulic similarity.

3. Results and Discussion

To quantitatively assess the hydraulic implications of coolant selection, a comparative analysis was performed under an identical thermal duty of 100 MW and an allowable temperature rise of 50 K. All fluids were evaluated within the same pipe geometry and operating configuration, ensuring that differences in hydraulic performance arise solely from thermophysical property variations.

The analysis proceeds in a stepwise manner. First, the required mass flow rate and resulting bulk velocity are examined to establish the fundamental thermal transport demand. Next, the flow regime and Reynolds number are evaluated to confirm the applicability of turbulent friction correlations. The resulting pressure drop and pump power are then compared to quantify the hydraulic penalty associated with each coolant. Finally, scaling behavior and sensitivity to allowable temperature rise are analyzed to derive practical pump design implications.

This structured comparison enables a consistent evaluation of molten salts relative to water, isolating the impact of specific heat capacity, density, and viscosity on overall pumping requirements.

3.1 Mass Flow and Velocity Requirement

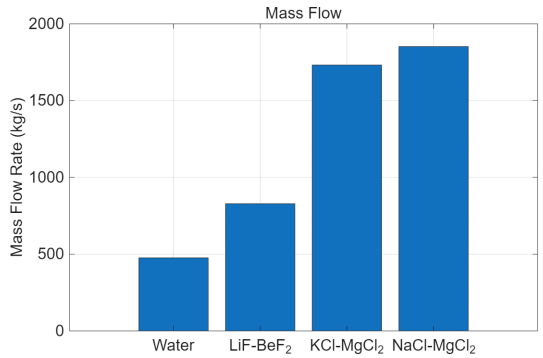

Fig. 2. Required mass flow rate for 100 MW_{th} heat removal at $\Delta T = 50$ K

Fig. 2 compares the required mass flow rates of the four candidate coolants under a fixed thermal duty of 100 MW and an allowable temperature rise of 50 K. A substantial variation is observed among the fluids, primarily due to differences in specific heat capacity.

Water requires approximately 4.76×10^{2}kg/s, representing the lowest flow demand. FLiBe requires 8.28×10^{2} kg/s, corresponding to a 74% increase relative to water. In contrast, the chloride salts demand significantly higher flow rates: 1.73×10^{3} kg/s for KCl–$MgCl_2$ and 1.85×10^{3} kg/s for NaCl–$MgCl_2$, which are approximately 3.6–3.9 times higher than that of water.

This increase in mass flow directly translates into higher volumetric flow rates. Despite their higher densities, the molten salts exhibit elevated bulk velocities compared to water due to the large mass flow demand. The increase in flow velocity is particularly critical because it directly affects hydraulic losses, which scale nonlinearly with velocity. Therefore, even at this preliminary stage, chloride salts indicate a substantially greater hydraulic burden compared to water.

3.2 Reynolds Number and Flow Regime Characterization

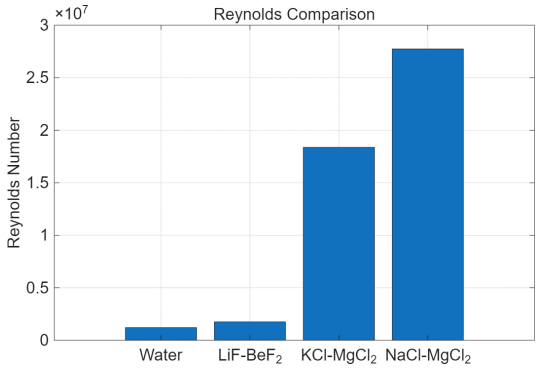

Fig. 3. Reynolds number comparison under reference condition.

Fig. 3 presents the Reynolds numbers for each coolant under the reference operating condition. All fluids operate within the fully turbulent regime, with Reynolds numbers exceeding 10^5 in all cases.

Water exhibits a Reynolds number on the order of 10^6, while FLiBe and the chloride salts fall within a similar magnitude range despite differences in viscosity. Notably, although chloride salts possess lower dynamic viscosities than water, their significantly higher velocities dominate the Reynolds number scaling, resulting in comparable or even elevated turbulence intensity.

The fully turbulent regime across all cases justifies the application of conventional turbulent friction correlations. More importantly, since all fluids share a similar flow regime, differences in hydraulic performance are primarily driven by density and velocity effects rather than regime transitions.

3.3 Pump Head and Hydraulic Power Requirement

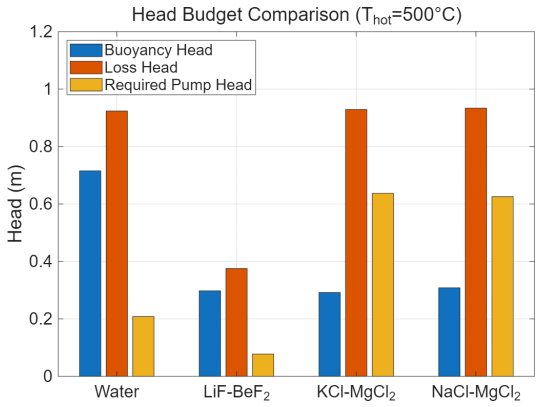

Fig. 4. Decomposition of hydraulic head and required pump head by coolant

Fig. 4 compares the frictional head loss, buoyancy head, and resulting required pump head for each coolant under the reference condition of 100 MW_{th} and $\Delta T = 50$ K.

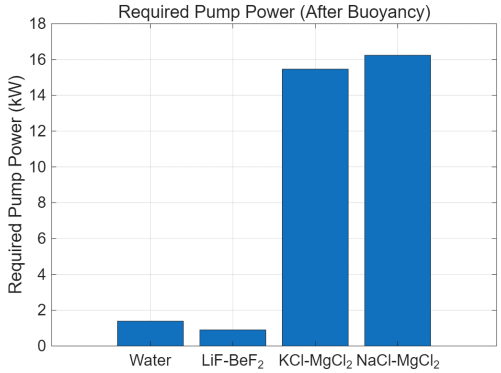

Fig. 5. Required pump power considering buoyancy effect (100 MW_{th}, ΔT = 50 K)

Fig. 5 presents the required pump power after accounting for buoyancy effects. Although buoyancy provides a measurable driving contribution, its magnitude remains significantly smaller than the frictional head loss for all fluids. As a result, the net pump requirement is primarily governed by velocity-dependent hydraulic resistance.

Water exhibits the lowest pump head and power, followed by FLiBe with a moderate increase. In contrast, the chloride salts require substantially higher pumping power due to their elevated mass flow rates and associated dynamic pressure effects. As illustrated in Fig. 6, the disparity becomes more pronounced on a logarithmic scale, highlighting the nonlinear amplification of hydraulic power with increasing flow demand.

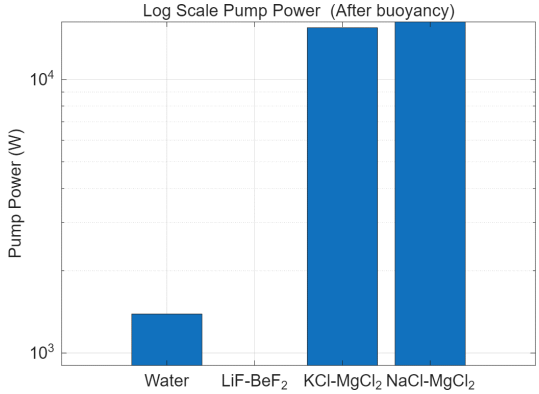

Fig. 6. Required pump power considering buoyancy effect on a logarithmic scale (100 MW_{th}, ΔT = 50 K)

The dominant mechanism underlying this increase is the elevated dynamic pressure associated with higher flow velocities. While molten salts possess higher densities that influence static pressure scaling, the quadratic dependence of frictional loss on velocity plays a more decisive role. As a result, the combined effect of increased mass flow and velocity amplification leads to a pronounced hydraulic power penalty.

From a system integration perspective, this translates into higher parasitic power consumption, reduced net plant efficiency, and potentially larger pump sizing requirements when chloride salts are employed.

3.4 Thermal Sensitivity to Allowable Temperature Rise

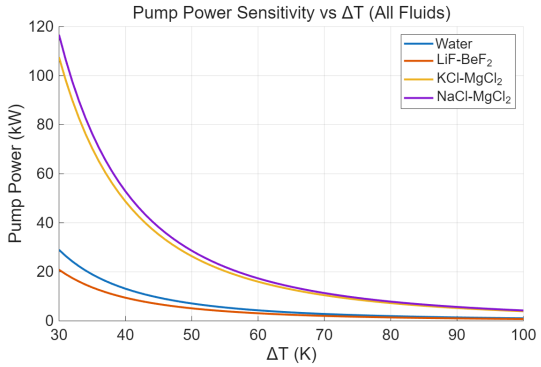

Fig. 7. Pump power sensitivity to allowable temperature rise (ΔT) at 100 MW_{th}

Fig. 7 presents the pump power as a function of allowable temperature rise ranging from 30 K to 100 K. A strong inverse relationship is observed for all fluids.

Increasing the temperature rise from 30 K to 100 K reduces pump power by more than a factor of three across all cases. The sensitivity is particularly pronounced for chloride salts, where pump power decreases sharply as ΔT increases. This behavior reflects the nonlinear dependence of hydraulic losses on mass flow rate.

These results indicate that allowable temperature rise is an effective design variable for mitigating hydraulic penalties in molten salt systems. By increasing ΔT, pumping requirements can be substantially reduced without modifying fluid composition or mechanical configuration.

For the water case, the analysis was conducted under the supercritical pressure condition defined in Section 2.1. Accordingly, the ΔT sensitivity results are interpreted within the single-phase supercritical operating regime.

3.5 Pump Scaling Requirements: Diameter and Rotational Speed

Fig. 8 and 9 compare the required impeller diameter ratio and rotational speed ratio relative to the water baseline. Molten salts demand either increased impeller diameter or elevated rotational speed to satisfy the higher flow and head requirements.

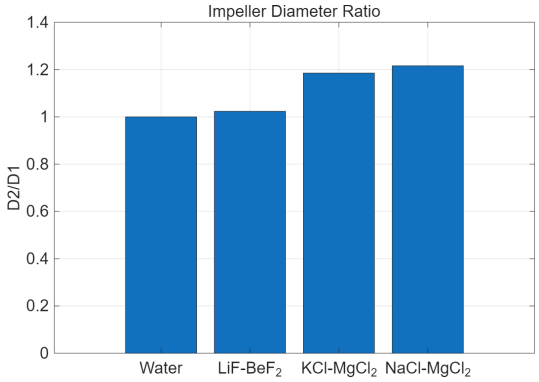

Fig. 8. Impeller diameter scaling relative to water (D_{salt}/D_{water})

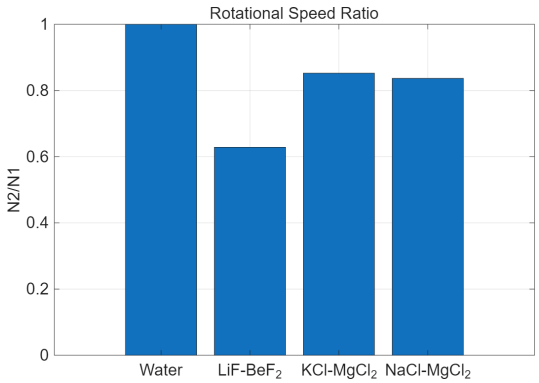

Fig. 9. Rotational speed ratio relative to water (N_{salt}/N_{water})

The chloride salts require significantly larger scaling adjustments compared to FLiBe. In practical terms, this translates into increased mechanical stress, potential vibration concerns, and higher material constraints. The scaling results indicate that while hydraulic requirements rise considerably, they remain within achievable centrifugal pump design limits.

3.6 Pump Power Iso-Contours and Design Envelope in N–D Space

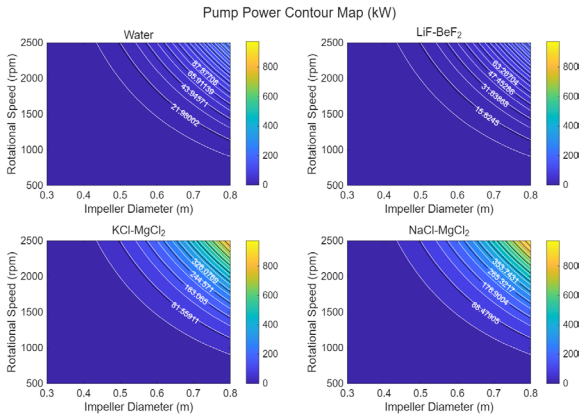

Fig. 10. Comparison of Pump Power Distribution in N–D Parameter Space

The contour maps shown in Fig. 10 illustrate the pump power distribution across rotational speed and impeller diameter space for each coolant. A clear shift toward higher power regions are observed for molten salts compared to water.

For chloride salts, achieving the required operating point necessitates either higher rotational speeds or larger impeller diameters, moving the design toward regions of increased mechanical loading. However, the contour topology remains consistent across fluids, indicating that the fundamental pump performance characteristics are preserved.

The N–D curves reveal a clear trade-off relationship, where increasing impeller diameter allows a proportional reduction in rotational speed while maintaining the required head. This geometric–kinematic flexibility offers a practical design margin for accommodating molten salt operation within acceptable mechanical limits.

This suggests that conventional centrifugal pump architectures remain applicable, albeit with modified geometric scaling.

3.7 Specific Speed and Pump Type Implication

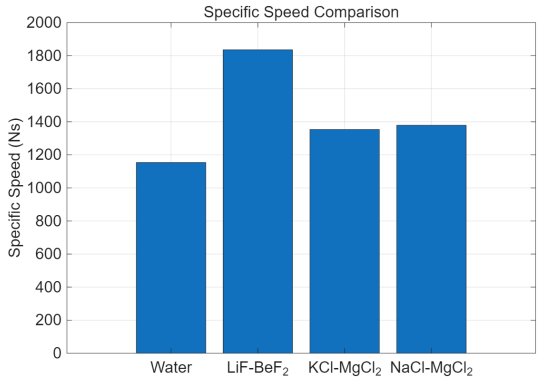

Fig. 11. Specific Speed Comparison at N = 1500 rpm

Fig. 11 presents the specific speed calculated at the reference rotational speed of 1500 rpm for each coolant. Despite the substantial differences in required mass flow rate and pump head, the resulting specific speeds fall within a relatively narrow range. It should be noted that the specific speed values reported here were evaluated at a fixed rotational speed of 1500 rpm to compare operating points under identical mechanical conditions. The analysis does not assume identical pump geometry across fluids; rather, it illustrates how the required operating point shifts as coolant properties vary.

Water exhibits a specific speed of approximately 1150, while FLiBe shows a higher value of approximately 1830. The chloride salts, KCl–$MgCl_2$ and NaCl–$MgCl_2$, yield intermediate values around 1350–1380. These values fall within the typical radial-flow centrifugal pump regime (generally $N_s \approx 500$–3000) [9, 10]. Although molten salts require significantly higher hydraulic power compared to water, the corresponding specific speeds remain within

the typical operating range of radial-flow centrifugal pumps.

This observation indicates that the transition from water to molten salts does not necessitate a fundamental change in pump type. Instead, the primary design implication lies in accommodating increased hydraulic loading and associated mechanical demands, rather than altering the overall pump configuration.
`

Overall, while molten salts impose a substantial hydraulic burden compared to water, the fundamental pump operating characteristics remain preserved under affinity-based scaling. The primary design challenge therefore lies in managing increased hydraulic loading rather than redefining pump architecture.

4. Conclusions

This study quantitatively evaluated the hydraulic implications of coolant selection for a 100 MW_{th} loop under identical geometric and operating conditions. Compared to water, chloride-based molten salts require approximately 3.6–3.9 times higher mass flow rates, leading to significantly increased pump head and power requirements due to nonlinear velocity-dependent pressure losses.

Sensitivity analysis revealed that allowable temperature rise is a critical design variable, capable of reducing pump power by more than a factor of three within practical operating limits. Affinity-based scaling analysis demonstrated that although molten salts shift the operating point toward higher rotational speeds or larger impeller diameters, the fundamental pump performance topology remains unchanged.

The calculated specific speeds indicate that conventional radial-flow centrifugal pumps remain suitable across all coolants. Therefore, the transition from water to molten salt cooling primarily necessitates mechanical and hydraulic scaling adjustments rather than fundamental changes in pump architecture.

ACKNOWLEDGEMENTS

This work was supported by the National Research Foundation of Korea (NRF) grant funded by the Korea government (MSIT) (No. RS-2025-25454059).

REFERENCES

[1] Dolan, T. J. (2024). *Molten salt reactors and thorium energy*. Elsevier Science & Technology.
[2] S. Choi, T. Min, I. W. Son, S. Yoo, and J. I. Lee, "Selecting Optimal Heat Transfer Chloride Salt for Molten Salt Fast Reactor," *Transaction of the Korean Nuclear Society Spring Meeting*, Jeju, Korea, May 18-19, 2023
[3] O'Brien, J. E., Sabharwall, P., Yoon, S. J., & Housley, G. K. (2014). *Strategic need for a multi-purpose thermal hydraulic loop for support of advanced reactor technologies* (No. INL/EXT--14-33300). Idaho National Lab.(INL), Idaho Falls, ID (United States).
[4] Wibisono, A. F., Ahn, Y., Williams, W. C., Addad, Y., & Lee, J. I. (2013). Studies of various single phase natural circulation systems for small and medium sized reactor design. *Nuclear engineering and design*, 262, 390-403.
[5] Williams, D. F. (2006). *Assessment of candidate molten salt coolants for the NGNP/NHI heat-transfer loop* (No. ORNL/TM--2006/69). Oak Ridge National Laboratory (ORNL), Oak Ridge, TN (United States).
[6] Sohal, M. S., Ebner, M. A., Sabharwall, P., & Sharpe, P. (2010). *Engineering database of liquid salt thermophysical and thermochemical properties* (No. INL/EXT-10-18297). Idaho National Laboratory (INL).
[7] Huber, M. L., Perkins, R. A., Laesecke, A., Friend, D. G., Sengers, J. V., Assael, M. J., ... & Miyagawa, K. (2009). New international formulation for the viscosity of H_2O. *Journal of Physical and Chemical Reference Data*, 38(2), 101-125.
[8] Stepanoff, A. J. (1957). *Centrifugal and axial flow pumps. Theory, design, and application*.
[9] Menon, E. S. (2009). *Working Guide to Pump and Pumping Stations: Calculations and Simulations*. Gulf Professional Publishing.
[10] Karassik, I., & McGuire, J. T. (Eds.). (2012). *Centrifugal pumps*. Springer Science & Business Media.